












SEISMIC DOMAIN IDENTIFICATION ALGORITHM USING FUZZY LOGIC METHODS WITH COMBINED GEOLOGICAL AND GEOMORPHOLOGICAL DATA FOR THE CASE OF SAKHALIN ISLAND

A. L. Sobisevich¹ , G. M. Steblov^{1,2} , A. O. Agibalov^{3,1} , I. M. Aleshin^{1,4} , G. R. Balashov¹ , A. D. Kondratov¹ , V. M. Makeev⁵ , V. P. Perederin¹ , F. V. Perederin¹ , A. A. Sentsov^{*,1} , and K. I. Kholodkov¹ 

¹Schmidt Institute of Physics of the Earth of the Russian Academy of Sciences, Moscow, Russia

²Institute of Earthquake Prediction Theory and Mathematical Geophysics of the Russian Academy of Sciences, Moscow, Russia

³Lomonosov Moscow State University, Moscow, Russia

⁴Geophysical Center of the Russian Academy of Sciences, Moscow, Russia

⁵Sergeev Institute of Environmental Geoscience of the Russian Academy of Sciences, Moscow, Russia

* **Correspondence to:** Alexey A. Sentsov, alekssencov@yandex.ru.

Abstract: An algorithm for identifying seismic generation zones or “seismic domains” using fuzzy logic has been developed and tested on the island of Sakhalin. Initial data were obtained from diagrams of the distribution of “weak” zones, relief elevation distribution skewness, and magnitude of recent area deformation for one year. These data were processed using a γ -operator in fuzzy logic with $\gamma = 0.9$, which allowed us to identify areas with high seismic activity. The areas where these active areas intersect with zones with increased compressive stress values, as determined by computer modeling, were considered to be seismic zones. It was shown that, if there are not enough source materials available, it is possible to exclude information about the recent deformation field from consideration and use an assumed grid of active faults for computer modeling. This approach may be useful when analyzing areas that have not been studied well.

Keywords: morphometric analysis of relief, fuzzy logic, neotectonics, seismotectonics, seismic domains, seismic generation zone, GNSS.

Citation: Sobisevich, A. L., G. M. Steblov, A. O. Agibalov, I. M. Aleshin, G. R. Balashov, A. D. Kondratov, V. M. Makeev, V. P. Perederin, F. V. Perederin, A. A. Sentsov, and K. I. Kholodkov (2024), Seismic Domain Identification Algorithm Using Fuzzy Logic Methods With Combined Geological and Geomorphological Data for the Case of Sakhalin Island, *Russian Journal of Earth Sciences*, 24, ES2004, EDN: JZBFTU, <https://doi.org/10.2205/2024es000906>

RESEARCH ARTICLE

Received: 5 March 2024

Accepted: 7 April 2024

Published: 6 May 2024



Copyright: © 2024. The Authors. This article is an open access article distributed under the terms and conditions of the Creative Commons Attribution (CC BY) license (<https://creativecommons.org/licenses/by/4.0/>).

Introduction

Currently, research is underway to formalize the methodology for identifying earthquake foci in different regions and to clarify lineament-domain focal models. This could be achieved by complex geological and geophysical data processing with a fuzzy logic algorithm [Dzeboev *et al.*, 2019; Gvishiani *et al.*, 2021; Kulchinsky *et al.*, 2010]. Due to the fact that a significant portion of the Russian Federation’s territory has not been sufficiently studied in terms of seismology, we have developed an algorithm for identifying areas that encompass homogeneous geological features and dissipated seismicity, which we call seismic generation zones here or “seismodomains”, “seismic domains” in Russian [Ulomov, 1987]. This is achieved by processing geological and geomorphological data using the fuzzy logic γ -operator. The effectiveness of this approach is justified by comparison with data on the modern seismic activity of Sakhalin Island, where during the instrumental observation period, more than 300 earthquakes have occurred with a depth up to 45 kilometers, including 13 that were sufficiently strong with magnitudes of $M \geq 5.5$.

Materials and Methods of Research

The initial data consisted of an Advanced Spaceborne Thermal Emission and Reflection Radiometer (ASTER) digital elevation model (DEM) with a resolution of 1 arc second (~ 30 m) [United States Geological Survey, 2023], river hydrography [Lehner and Grill, 2013] and a database of active faults [Zelenin et al., 2022]. The DEM and hydrography were used to calculate morphometric relief parameters, which are related to the nature of neotectonic movements. These parameters include: 1) density of “weak” zones, identified by the method [Kostenko, 1999]. 2) elevation distribution skewness. 3) steepness of slopes. 4) absolute curvature of the relief. 5) The difference between the basic surfaces of the 2nd and 3rd orders. 6) average elevation. 7) difference between the base surfaces of the 1st and 2nd orders. 8) difference in the of the relief elevation and the base surface of the 3rd order. 9) depth of vertical dissection. Seismically active zones have been identified according to their positive anomalies, where the corresponding values exceed the median or third quartile. In these zones, more than half of earthquake epicenters (for the median) or more than a quarter of earthquake epicenters (for the third quartile) are located (see Table 1). Calculations of skewness, average elevation, and depth of vertical dissections were performed using a 15×15 km grid.

Due to the fact that the current stress-strain state determines the nature of seismicity, the values of the areal deformation (ε_S) of the covering elements were calculated. These covering elements are Delaunay triangles [Delone, 1934], the vertices of which correspond to the global navigation satellite system (GNSS) points. Data on the location, velocity and direction of displacement of the latter are given in [Gridchina et al., 2023]. The values of ε_S are determined by the formula $\varepsilon_S = \frac{S_2 - S_1}{S_1}$, where S_1 is the area of the triangle, S_2 is the area of the triangle but with annual displacement of its vertices accounted.

Table 1. The relationship of positive anomalies of morphometric parameters of the relief of the Sakhalin Island with modern seismicity

Morphometric parameters of the relief	The proportion of earthquake epicenters located in the areas where the values of the morphometric parameter $\geq Q2$	The proportion of earthquake epicenters, where the values of the morphometric parameter $\geq Q3$
1	0.62	0.35
2	0.57	0.31
3	0.51	0.29
4	0.51	0.28
5	0.54	0.27
6	0.55	0.22
7	0.56	0.28
8	0.54	0.25
9	0.58	0.23

Note: Q2 – the median, Q3 – the 3rd quartile. The numbers indicate: 1) density of “weak” zones, identified by the method [Kostenko, 1999]. 2) elevation distribution skewness. 3) steepness of slopes. 4) absolute curvature of the relief. 5) The difference between the basic surfaces of the 2nd and 3rd orders. 6) average elevation. 7) difference between the base surfaces of the 1st and 2nd orders. 8) difference of the relief elevation and the base surface of the 3rd order. 9) depth of vertical dissection.

The analysis of morphometric parameters of the relief and the modern deformation pattern by fuzzy logic was performed using the γ -operator [Zimmermann, 2001] in the ArcGIS environment. The corresponding bitmaps were transformed by a linear algorithm and stacked-up into fuzzy sets. Then, we use the fuzzy gamma function: $\mu(x) = (\mu_{\text{Sum}})^\gamma \times (\mu_{\text{Product}})^{(1-\gamma)}$, where γ are set in the range from 0 to 1, μ_{Sum} – fuzzy set sum, and μ_{Product} – fuzzy set product. If the value of γ is close to 1, then the result is close to the fuzzy sum, and vice versa: if γ is close to 0, then the result is close to the fuzzy

product. Assuming that this gamma function is parametrized with relief morphometrics and modern horizontal displacement indicators we apply this function to each cell to acquire the neotectonics activity index I . The values of γ equal to 0.25, 0.50, 0.75 and 0.90 were tested.

Confidence analysis was performed with Receiver operating characteristic (ROC) binary classification method parametrized with integral parameter I and earthquake epicenter map. Each dataset was gridded with cell size of 15×15 km and adjusted. Thus, each cell was assigned with two values: maximum integral parameter I and 1-or-0 value of earthquake epicenter(s) presence, zero being not.

In addition, the proposed algorithm for isolating seismic generation zones involves the use of the results of computer geodynamic modeling, which allows us to identify areas with increased relative compressive stress values. The methodology of the algorithm and the results obtained for Sakhalin Island are described in [Steblov et al., 2023]. It should be noted that the scheme of active faults, as given in [Zelenin et al., 2022], was used as initial data. Due to the fact that the active faults in a number of regions in Russia have not been studied sufficiently, we use the example of Sakhalin to assess the effectiveness of their identification by DEM according to the method of Y. V. Nechaev [Nechaev, Yu. V., 2010]. This method involves determining the degree of tectonic fragmentation by the specific length of the “weak” zones within a cell with side a for a depth of $h = a/2$. The specific length of these “weak” areas is calculated as the ratio of the total length of these areas to the area of the cell (a^2). By varying the values of a , the degree of fragmentation was estimated in the depth range of 2.5–20 km and the vertical profiles were compared for this parameter with data on active faults.

Results and Discussion

As the most informative parameters, 2 morphometric parameters were selected – the density of “weak” zones and the skewness of relief elevation distribution. These parameters are based on the number of earthquake epicenters falling into areas where the values of these parameters exceed the median (Q2) or the 3rd quartile (Q3). The proportion of earthquake epicenters located within areas contoured by values $\geq Q3$ is 0.35 for density of “weak” zones and 0.31 for elevation distribution skewness, respectively. This exceeds similar values for other morphometric characteristics that were considered. Additionally, during the transition from Q2 to Q3, the proportion of epicenters decreases by less than a factor of 2 (see Table 1). In general, areas with positive values of elevation distribution skewness have a high potential energy in the relief, while areas with increased density of weak zones correspond to regions where brittle deformations occur (Figure 1).

At the first stage, three parameters were processed by the γ -operator – the density of “weak” zones, the elevation distribution skewness, and the magnitude of modern dilation at $\gamma = 0.9$ (Figure 2B). The choice of this gamma value is due to the fact that it provides the largest range of values for estimating the degree of belonging of parameter I to set μ . Seismically active regions are characterized by elevation values of I from 0.6 to 0.9, occupying 47% of the studied area. This is 19% less than the entire island, due to the lack of data on the values for its northern and southern extremities. 44% of epicenters fall within these limits, including 70% with $M_w \geq 5.5$, while 78% of events and 92% of high magnetic events fall within the uncertainty zone, which varies from 0.4 to 0.6 at this stage. At the second stage, a simplified methodology for allocating seismically active areas was tested. In this case, with $\gamma = 0.9$, only two parameters were processed: the density of “weak” zones and elevation distribution skewness. It was discovered that 47% of epicenters, including 30% of earthquakes with $M_w \geq 5$, occur in areas with elevated values of I (between 0.6 and 0.9) that occupy 66% of the area of the island (Figure 2C). The reliability of these models was confirmed through ROC analysis. The first model’s prognostic accuracy was analyzed for both all earthquakes (Figure 3I) as well as events with $M \geq 5.5$ (Figure 3II). For the first case, Area Under the Curve (AUC) value is 0.60 and for the latter it is 0.70. For the second, the corresponding values are 0.66 and 0.86 (Figures 3III and 3IV).

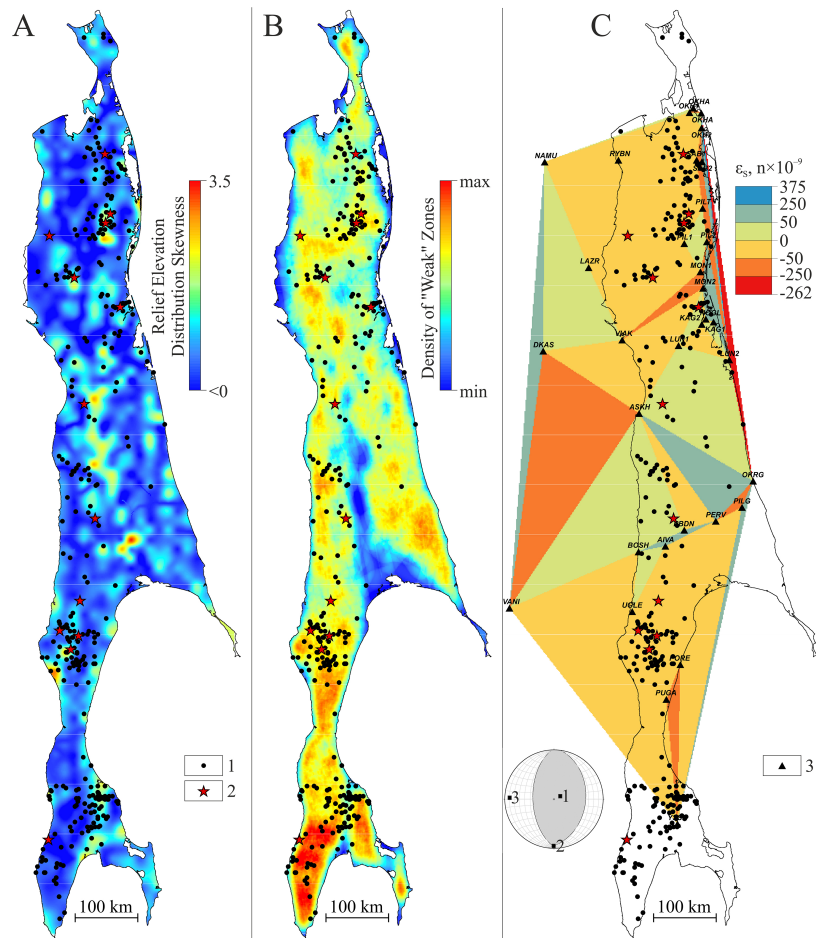


Figure 1. Mapped parameters derived of initial data for the analysis with the γ -operator: relief elevation distribution (A), density of “weak” zones (B) and modern areal deformation (ϵ_S) of the island of Sakhalin (C). 1–2 – epicenters of earthquakes with magnitude: 1 – $M < 5.5$; 2 – $M \geq 5.5$; 3 – GNSS points. In the round inset on C we show the reconstruction of the main normal stress axes by Y. L. Rebetsky method of cataclastic analysis of discontinuous displacements for focal mechanisms of earthquake foci [Rebetsky, Yu. L. et al., 2017] (lower hemisphere): 1–3 are the main normal stress axes: 1 – stretching, 2 – intermediate, 3 – compression.

Compressive stresses predominate on Sakhalin Island, as evidenced by the nature of the field of modern area deformation. This is confirmed by the reconstruction of the main normal stress axes by Y. L. Rebetsky method of cataclastic analysis of discontinuous displacements for focal mechanisms of earthquake foci [Rebetsky, Yu. L. et al., 2017] (Figure 1C, inset). Overall, the configuration of seismically active areas identified by increased I values is consistent with the contours of areas of compressive stress localization previously established by computer geodynamic modeling [Steblov et al., 2023]. The zones with increased relative compressive stress values, where the calculated I ranges from 0.6 to 0.9 for 3 parameters, are considered here as seismic generation zones. This approach validates the allocation of all previously identified seismic generation zones (Figure 2D, I–VI in Table 2), as described in [Steblov et al., 2023] and also allows for the identification of 5 new seismic generation zones (Figure 2D, VII–XI in Table 2). Estimates of the maximum magnitude of the expected earthquake for each domain were made according to RB-019-18 [2018] by adding 0.5 magnitude units to the magnitude of the strongest known earthquake. The exception is seismic generation zone XI, where no seismic events were recorded during the entire observation period. However, based on the results we obtained, it is considered an area where earthquakes with $M \geq 5.5$ are possible. It should be noted that the proposed seismic domain model is consistent with the Lineament Domain Model IMGIG-97 [Oskorbin, 1997], complementing and clarifying it.

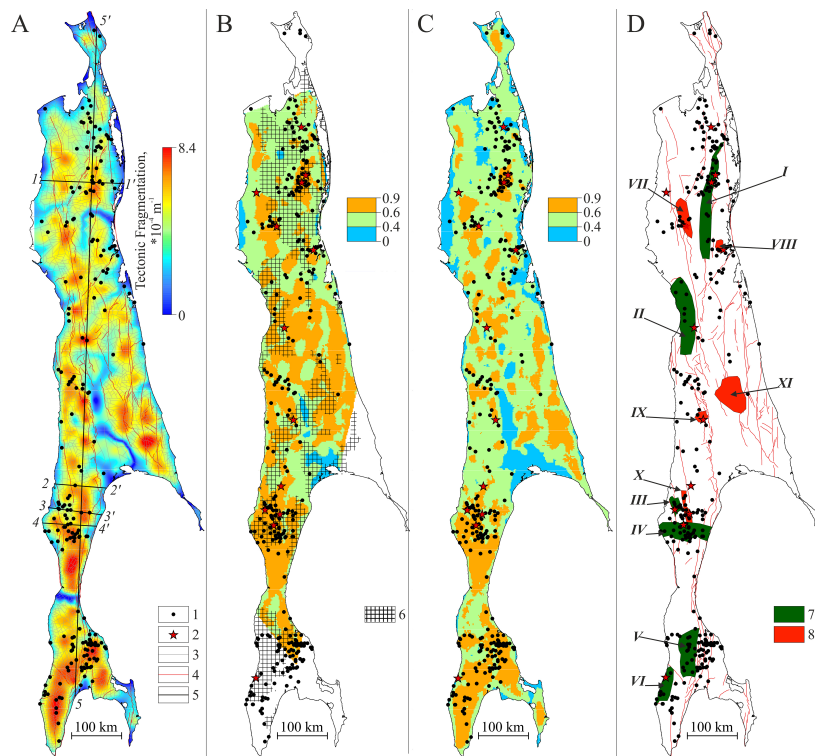


Figure 2. Map of tectonic fragmentation of Sakhalin (A), the results of processing by the γ -operator with GNSS (B) and without GNSS data (C), seismic generation zones (D). 1–2 – epicenters of earthquakes with magnitude: 1 – $M < 5.5$; 2 – $M \geq 5.5$; 3 – “weak” zones; 4 – active discontinuous disturbances, according to [Zelenin et al., 2022]; 5 – the position of tectonic fragmentation profiles; 6 – areas of localization of maximum compressive stresses, according to [Steblov et al., 2023]; 7 – seismic generation zones, according to [Steblov et al., 2023]; 8 – seismic generation zones highlighted by the algorithm considered in the text.

Table 2. Estimation of the maximum expected magnitude (M_{max}) within the limits of the Sakhalin Island seismic generation zones

Seismic Generation Zone Number	M_{max}
I	8
II	6.1
III	6.8
IV	7.6
V	5.5
VI	6.7
VII	6.1
VIII	6.1
IX	6.1
X	6
XI	5.5

The construction of vertical sections of the tectonic fragmentation field (Figure 2A, Figure 4) showed that most of the active faults considered in [Zelenin et al., 2022] are manifested in them. The 5 profile lines in Figure 2A show between 60 and 80% active faults with an average of 74%. This result shows that with an insufficient level of insight to use data on suspected active faults identification using method as in [Delone, 1934] one can use the Y. V. Nechaev method [Nechaev, Yu. V., 2010] with DEM data.

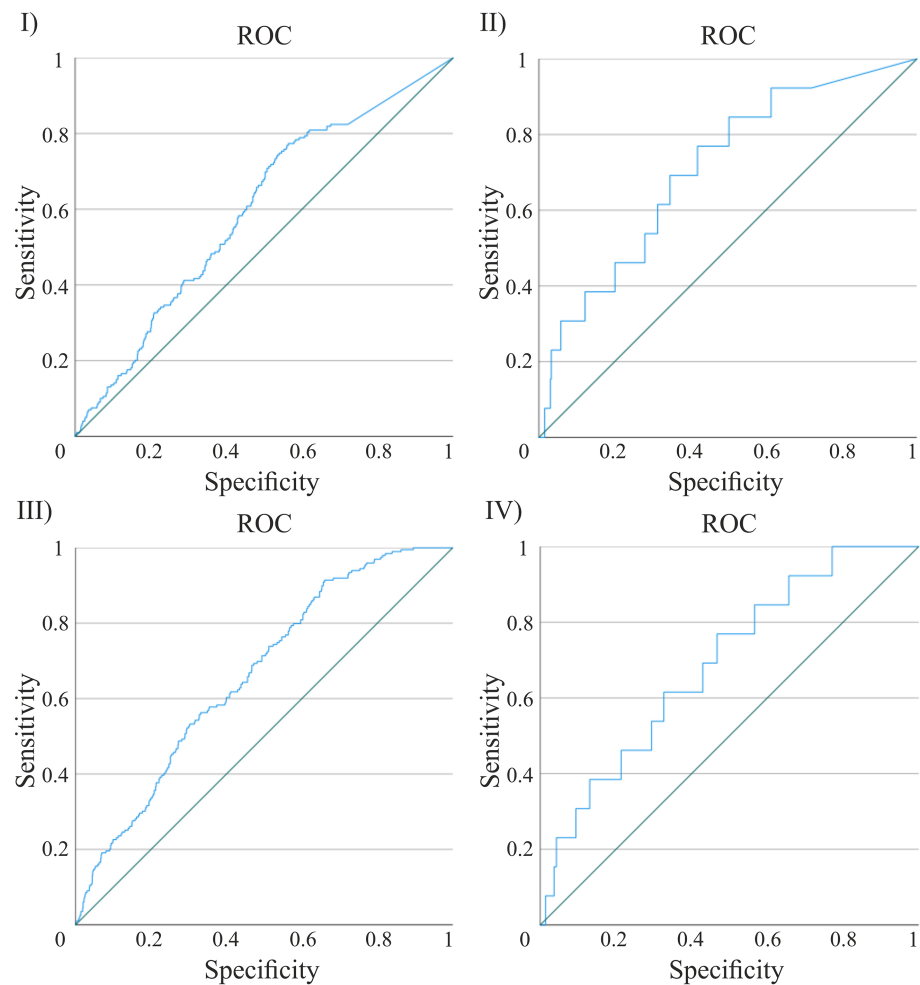


Figure 3. ROC curves (blue lines) constructed for the neotectonic activity index (I) and earthquake epicenters of Sakhalin Island: I–II for the first model (explanations in the text): – I taking into account the entire magnitude range under consideration, II – only for earthquakes with $M \geq 5.5$; III–IV – for the second model: III – taking into account the entire considered range of magnitudes, IV – only for earthquakes with $M \geq 5.5$. Diagonal lines are the boundaries of a random distribution. Specificity and sensitivity are two important characteristics of an algorithm. Specificity refers to the ability of the algorithm to accurately identify objects in a sample that have a specific feature, while sensitivity refers to its ability to differentiate between objects that have and do not have the same feature [Belyaev *et al.*, 2023].

Conclusion

We have proposed an algorithm for identifying seismic generation zones. It involves analyzing 3 parameters: the density of “weak” zones; elevation distribution skewness; and values of modern areal deformation. We use the γ -operator from fuzzy logic to analyze these parameters and compare them with the configuration of areas with increased relative values of compressive stress, which were identified by computer modeling. It is shown that, without initial data, an analysis of only 2 parameters can be acceptable (without considering modern areal deformations). It is also possible to carry out modeling using information on potential active faults identified using the Y. V. Nechaev method [Nechaev, Yu. V., 2010] with DEM data. The testing of this algorithm using the example of Sakhalin Island has shown its effectiveness and allowed us to expand our knowledge of the configuration of seismic zones or, in Russian, “seismodomains”.

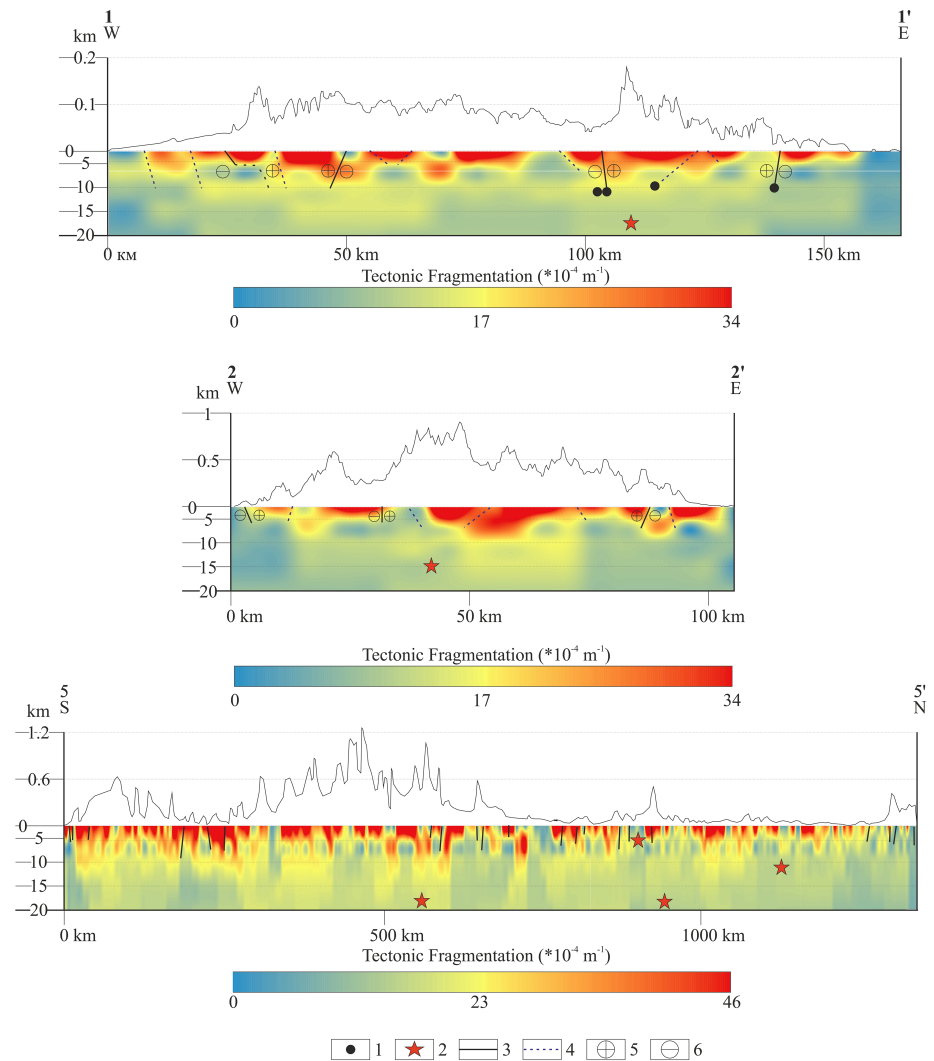


Figure 4. Profiles of tectonic fragmentation (Figure 2A) through the foci of the Neftegorsky (1–1′) and Ulegorsky (2–2′) earthquakes, and through the entire Sakhalin Island (5–5′). 1–2 – hypocenters of earthquakes with magnitude: 1 – $M < 5.5$, 2 – $M \geq 5.5$; 3 – faults [Zelenin et al., 2022] as seen from tectonic fragmentation perspective; 4 – “weak” zones as seen from tectonic fragmentation perspective; 5 – upthrown block of the fault; 6 – downthrown block.

Acknowledgements. This study was conducted as part of the state assignment of the IPE RAS (#075-01030-23), the state assignment of the IEPT RAS (#075-00605-24-00), the state assignment of the GC RAS (#075-01349-23-00), the state assignment of the IGE RAS (#122022400105-9) and the research project “Modeling of the latest geodynamic processes affecting seismicity and fluid permeability of sedimentary strata” (MSU named after M. V. Lomonosov).

References

- Belyaev, A. M., A. E. Mikhlin, and M. V. Rogachev (2023), *ROC analysis and logical regression in MedCalc*, 36 pp., National Medical Research Center of Oncology named after N. N. Petrova (in Russian).
- Delone, B. N. (1934), On the emptiness of the sphere, *Izvestiya Akademii Nauk SSSR*, (4), 793–800 (in Russian).
- Dzeboev, B. A., A. D. Gvishiani, I. O. Belov, V. N. Tatarinov, S. M. Agayan, and Yu. V. Barykina (2019), Strong-Earthquake-Prone Areas Recognition Based on an Algorithm with a Single Pure Training Class: I. Altai-Sayan-Baikal Region, $M \geq 6.0$, *Physics of the Earth*, (4), 33–47, <https://doi.org/10.31857/S0002-33372019433-47> (in Russian).

- Gridchina, M. S., G. M. Steblov, I. S. Vladimirova, and A. V. Basmanov (2023), Investigation of the Lithospheric Plate Boundary Zone within Sakhalin Island Based on Satellite Geodesy Data, *Geophysical Research*, 24(4), 81–96, <https://doi.org/10.21455/gr2023.4-5> (in Russian).
- Gvishiani, A. D., B. A. Dzeboev, S. M. Agayan, I. O. Belov, and J. I. Nikolova (2021), Fuzzy Sets of High Seismicity Intersections of Morphostructural Lineaments in the Caucasus and in the Altai-Sayan-Baikal Region, *Journal of Volcanology and Seismology*, 15(2), 73–79, <https://doi.org/10.1134/s0742046321020032>.
- Kostenko, N. P. (1999), *Geomorphology*, 379 pp., Moscow University, Moscow (in Russian).
- Kulchinsky, R. G., E. P. Kharin, I. P. Shestopalov, A. D. Gvishiani, S. M. Agayan, and S. R. Bogoutdinov (2010), Fuzzy logic methods for geomagnetic events detections and analysis, *Russian Journal of Earth Sciences*, 11, RE4003, <https://doi.org/10.2205/2009ES000371> (in Russian).
- Lehner, B., and G. Grill (2013), Global river hydrography and network routing: baseline data and new approaches to study the world's large river systems, *Hydrological Processes*, 27(15), 2171–2186, <https://doi.org/10.1002/hyp.9740>.
- Nechaev, Yu. V. (2010), *Lineaments and tectonic fragmentation: remote sensing of the internal structure of the lithosphere*, 215 pp., IPE RAS, Moscow (in Russian).
- Oskorbin, L. S. (1997), Seismogenic zones of Sakhalin and adjacent regions, *Problems of seismic hazard of the Far Eastern region*, pp. 157–178 (in Russian).
- RB-019-18 (2018), Safety Guide to the Use of Atomic Energy “Assessment of the Initial Seismicity of the Area and Site of a Nuclear Energy Use Object During Engineering Surveys and Research” (in Russian).
- Rebetsky, Yu. L., L. A. Sim, and A. V. Marinin (2017), *From slip surfaces to tectonic stresses. Methods and algorithms*, 234 pp., GEOS, Moscow (in Russian).
- Steblov, G. M., A. O. Agibalov, V. M. Makeev, V. P. Perederin, F. V. Perederin, and A. A. Sentsov (2023), On the problem of estimation of the maximum possible earthquake magnitudes on Sakhalin island by various methods, *Problems of Engineering Seismology*, 50(4), 25–35, <https://doi.org/10.21455/vis2023.4-2> (in Russian).
- Ulomov, V. I. (1987), Lattice model of focal seismicity and forecast of seismic hazard, *Uzbekistan Geological Journal*, (6), 20–25 (in Russian).
- United States Geological Survey (2023), Search Data Catalog, https://lpdaac.usgs.gov/product_search/?collections=MEaSURES+SRTM&status=Operational&view=list, (date of access: 01.01.2023).
- Zelenin, E., D. Bachmanov, S. Garipova, V. Trifonov, and A. Kozhurin (2022), The Active Faults of Eurasia Database (AFEAD): the ontology and design behind the continental-scale dataset, *Earth System Science Data*, 14(10), 4489–4503, <https://doi.org/10.5194/essd-14-4489-2022>.
- Zimmermann, H.-J. (2001), *Fuzzy Set Theory - and Its Applications*, 435 pp., Springer Netherlands, <https://doi.org/10.1007/978-94-010-0646-0>.